Catalysis Today 179 (2012) 27–34

Contents lists available at ScienceDirect

Catalysis Today

journal homepage: www.elsevier.com/locate/cattod

Use of different templates on SAPO-34 synthesis: Effect on the acidity and catalytic activity in the MTO reaction

Teresa Álvaro-Muñoz, Carlos Márquez-Álvarez, Enrique Sastre*

Instituto de Catálisis y Petroleoquímica, ICP-CSIC, C/Marie Curie, 2, 28049 Madrid, Spain

ARTICLE INFO

Article history:
Received 30 May 2011
Received in revised form 18 July 2011
Accepted 25 July 2011
Available online 31 August 2011

Keywords:
SAPO-34
Structure directing agents
Methanol-to-olefins

ABSTRACT

SAPO-34 molecular sieves have been synthesized with different structure directing agents. Although materials with the same framework structure (CHA type) are obtained in all cases, they possess different physicochemical properties, especially textural parameters and crystal size. These catalysts have been tested in the MTO process. All the samples exhibited high activity and selectivity to short chain olefins at the initial stages of the reaction, but they deactivate rapidly with time on stream, especially at high space velocity. It has been observed an important influence of the external surface, crystal size and acidity on the activity, selectivity and lifetime of the different samples. Thus, the sample synthesized with tetraethylammonium hydroxide as structure directing agent rendered the best catalytic performance owing to its higher external surface, smaller crystal size and higher acidity.

1. Introduction

The increasing demand for olefins has renewed the interest in the methanol-to-olefins (MTO) process as a route to obtain these valuable petrochemicals from carbon sources alternative to petroleum. Methanol can be efficiently produced from syngas obtained by natural gas reforming or carbon gasification, and it might even provide an environmentally carbon neutral alternative to fossil carbon sources [1], if produced by chemical recycling of carbon dioxide via hydrogenation [2] or from syngas obtained by biomass gasification [3]. This reaction is efficiently catalysed by various solid acids. The conversion of methanol over medium-pore zeolites (such as ZSM-5) normally produces extensive amounts of aromatics and paraffins (MTG process), and in the case of large-pore zeolites, rapid coke formation [4–6]. On the contrary, small-pore molecular sieves generate higher proportion of C_2–C_4 olefins, due to the diffusion properties and dimensions of the cavities of zeolitic materials (because if bulkier species are formed internally, they cannot diffuse out). However, the porous structure is not the only factor that determines the high selectivity to C_2–C_4 olefins, as high selectivities to light paraffins (mainly propane) can also be obtained with small-pore size zeolites. Decreasing the concentration of strong acid sites, which are responsible for hydrogen transfer reactions, is a key factor in reducing the conversion of olefins into paraffins. The methods used to reduce the concentration of strong acid sites on zeolites (and thus avoid these hydrogen transfer reactions) are dealumination, cation exchange and isomorphous substitution of aluminium by other trivalent cations.

The conditions of synthesis, cation exchange and dealumination seem to be very important to obtain catalysts that can function effectively in the conversion of methanol into light olefins. Moreover, the ratio between the number of acid sites in the external surface and those located on the intracrystalline pore surface plays an important role in this reaction. Therefore, the reaction yields are affected by the crystal size, for the external to internal acid sites ratio increases with decreasing the size of the crystals.

Silicoaluminophosphate materials (SAPO) have a mild acidity and, therefore, they present a very interesting alternative to obtain high selectivity towards light olefins in the MTO process. Zeolite-type small-pore microporous silicoaluminophosphate SAPO-34 (chabazite type of structure) has been proven an excellent catalyst for the MTO process, showing exceptionally high selectivity to lower olefins, with reported selectivities to C_2–C_4 olefins over 80% [7–10].

It is well known that templates play important roles in the synthesis of molecular sieves (structure-directing, space filling and charge compensation roles) [11,12]. One template may produce molecular sieves with different structures if the synthetic conditions are varied; in addition, one type of molecular sieve can also be synthesized with different organic templates [11]. The physicochemical properties of a given molecular sieve may also change with the use of different templates. In consequence, the catalytic performance of the materials could be different. Some years ago, Vomscheid et al. [13] demonstrated that, in the synthesis of SAPO-34 with morpholine and TEAOH, the importance of the template appears not only in its role of directing the structure but also of

* Corresponding author.
E-mail address: esastre@icp.csic.es (E. Sastre).

0920-5861/$ – see front matter © 2011 Elsevier B.V. All rights reserved.
doi:10.1016/j.cattod.2011.07.038

Table 1
Gel composition and experimental synthesis conditions for the different SAPO-34 materials.

Catalyst	Synthesis gel composition (molar basis)	pH	Temperature (K)	Time (h)
S-1	$1Al_2O_3:0.8P_2O_5:0.6SiO_2:50H_2O:3TEA$	10.3	473	120
S-2	$1Al_2O_3:1P_2O_5:0.6SiO_2:30H_2O:1TEAOH$	6.8	423	120
S-3	$1Al_2O_3:1P_2O_5:0.6SiO_2:40H_2O:1TEAOH:0.6MA$	6.8	443	48
S-4	$1Al_2O_3:1P_2O_5:0.6SiO_2:20H_2O:2DPR$	7.3	473	120
S-5	$1Al_2O_3:0.8P_2O_5:0.6SiO_2:50H_2O:2DEA$	7.0	473	120

governing the distribution of Si in the framework, which clearly affects the catalytic properties of the samples. In a previous paper, Wilson and Barger [8], studied the synthesis of SAPO-34 with TEAOH and determined the influence of the different characteristics which affect the catalytic performance in the MTO process, i.e. shape selectivity, acid site strength, acid site density, particle size and Si content. Lee et al. [14] have observed that it is possible to vary the morphology and crystal size of SAPO-34 catalysts by using a mixture of morpholine and TEAOH as the synthesis template. When the mixture is used for the synthesis of SAPO-34, the crystal size is decreased to sub-micrometer size and the morphology of the particles is changed to spherical type formed by aggregation of nano-sized crystals. Although all the SAPO-34 catalysts showed similar activity and product distribution in the MTO reaction, the catalyst obtained using the mixture of 75% morpholine and 25% TEAOH exhibited a lifetime five times longer than that of the catalyst synthesized with 100% morpholine. In this sense, very recently, Ye et al. [15] have also studied the synthesis of SAPO-34 by hydrothermal method using different combinations of TEAOH and DEA as template. They obtained typical cubic shape SAPO-34 crystals, which size increased with the content of DEA in the gel. The authors concluded that the nature of the template used in the synthesis determines the morphology of final crystals because it influences the rate of crystal growth. In MTO conversion, the catalyst obtained using the mixture of 50% TEAOH and 50% DEA gave the longest lifetime due to optimal crystal size. Other authors [16] have described the synthesis of pure SAPO-34 using DEA as a template. Those catalysts presented a good catalytic performance in MTO reaction and a maximum of 81.5% selectivity to light olefins ($C_2H_4 + C_3H_6$) with 100% methanol conversion was obtained. It was also observed that an increase of the silicon content in SAPO-34 synthesized with DEA produced a gradual decrease in the catalysts lifetime and olefins selectivity.

Although some other papers have reported on the influence of the template in the catalytic properties of SAPO-34 for MTO [17–21] a systematic comparison of the physicochemical properties of the catalysts was not carried out. In this sense, the aim of this paper is the analysis of the effect that different templates used to synthesize SAPO-34 has on the parameters which affect the catalytic properties of these materials in the MTO reaction, namely silicon incorporation into the framework, acidity and crystal size.

2. Experimental

2.1. Synthesis of SAPO-34 molecular sieves

SAPO-34 catalysts were synthesized by a hydrothermal method using different organic templates at temperatures ranging 423–473 K. The molar composition of the reaction mixtures and the synthesis conditions for the different SAPO-34 materials obtained are given in Table 1.

Pseudoboehmite or aluminium hydroxide hydrate, 85% phosphoric acid and silica sol (30%) were used as sources of the framework elements. Different amines and derivatives have been used in the synthesis experiments as structure directing agents (SDA): triethyl amine (TEA), tetraethyl ammonium hydroxide (TEAOH), methylamine (MA), dipropyl amine (DPR) and diethyl amine (DEA). Experimental conditions (temperature and crystallization times) have been adjusted in order to obtain pure phases of SAPO-34 in all the cases. The same silicon to aluminium ratio (0.6) was used for all the synthesis gels prepared with different templates.

In a typical synthesis to get pure SAPO-34, the aluminium source – pseudoboehmite or aluminium hydroxide – was added slowly to a dilute phosphoric acid solution, and the mixture was vigorously stirred for 2 h to obtain a uniform gel. Silica solution was then added dropwise to this mixture followed by addition of the template. Finally, the mixture was stirred for about 4 h. The gel was then transferred into Teflon-lined stainless steel autoclaves with a capacity of 40 cm^3, which were heated statically at the required temperature under autogeneous pressure for the specified period of time.

The resulting solids were collected by centrifugation, washed with water and ethanol and dried at room temperature overnight. The organic template and the water trapped within the micropores of the as-synthesized solids were removed by calcination at 823 K prior to catalyst testing. Complete removal of the organic molecule was assessed by thermogravimetric analysis.

2.2. Characterization

Powder X-ray diffraction (XRD) patterns of as-synthesized and calcined samples were recorded on a Philips X'PERT diffractometer using CuK_α radiation with a nickel filter. The textural data (pore volume and BET surface area) were determined by nitrogen adsorption measurement using a Micrometrics ASAP 2010 volumetric apparatus. Previous to measure the nitrogen adsorption/desorption isotherms samples were degassed at 623 K under vacuum for at least 20 h. The crystal size morphology was analysed by scanning electron microscopy (SEM) using a JEOL JSM 6400 or a Philips XL30 microscopes, both operating at 20 kV.

The organic content of the samples was studied by elemental analysis with a Perkin-Elmer 2400 CHN analyser and by thermogravimetric analysis (TGA) using a Perkin-Elmer TGA7 instrument. TG analyses were carried out at a heating rate of 20 K/min under air flow. Elemental analysis for Al, P and Si was done for calcined samples by inductively coupled plasma optical emission spectrometry (ICP-OES, Perkin-Elmer 3300DV instrument) after sample dissolution by alkaline fusion.

For FTIR measurements, the powdered samples were pressed into self-supporting pellets and placed in a quartz cell, which allows thermal treatments in a vacuum. The samples were activated under vacuum (10^{-1} Pa) increasing the temperature slowly from 393 K to 823 K in the quartz cell used for FTIR measurements. CO was dosed on the pre-activated samples at a nominal temperature of 77 K. Then, the pressure of CO was reduced to obtain a sequence of FTIR spectra with different coverage. Spectra were collected on a Brucker FTIR 66 spectrometer equipped with a MCT cryodetector working at 2 cm^{-1} resolution, and normalized to a pellet thickness of 4 mg/cm^2. It was verified that the normalized spectra of all samples showed similar intensity of the framework vibrations combination bands in the region 1800–2000 cm^{-1}.

^{29}Si CP/MAS NMR spectra were recorded at room temperature using a Bruker AV-400-WB spectrometer operating at 79.5 MHz, with a 4 mm probe spinning at 10 kHz. A $\pi/2$ pulse of 3 μs, contact time of 6 ms and recycle delay of 5 s was used. The chemical shifts were referenced to tetramethylsilane (TMS).

2.3. Catalyst testing

Methanol conversion to olefins was tested at 673 and 723 K in a laboratory scale reactor set-up with a continuous down flow packed bed reactor fully automated and controlled from a personal computer (PiD Eng&Tech Microactivity Reference), operating at atmospheric pressure. Catalyst weight (between 0.5 and 1.0 g; 20–30 mesh pellets size) and methanol flow rate (0.150–0.025 ml/min) were varied in order to obtain different weight hourly space velocities (WHSV) between 1.2 and 14.2 h^{-1}. Previous to the reaction, samples were pre-treated under nitrogen flow at 723 K for 1 h. During the reaction, nitrogen was used as an inert diluent gas and co-fed with methanol into the reactor with a constant methanol/nitrogen ratio of 1/1 mol. The reaction products were analysed on-line by gas chromatography using a Varian CP3800 gas chromatograph equipped with flame ionization (FID) and thermal conductivity (TCD) detectors, with a Petrocol DH50.2 capillary column and a Porapack Q 80-100 mesh packed column for separation of hydrocarbons and oxygenates, respectively.

3. Results and discussion

3.1. Crystalline and morphological analysis

The X-ray powder diffraction patterns of the as-synthesized samples (Fig. 1) confirmed the structure type SAPO-34 (CHA structure) in all the materials. The patterns and peak positions match the patterns reported for this structure [17]. Practically no loss in crystallinity was observed when the as-synthesized samples were heated at 823 K in order to remove the organic molecules (Supplementary information, Fig. I), confirming their thermal stability under calcination conditions.

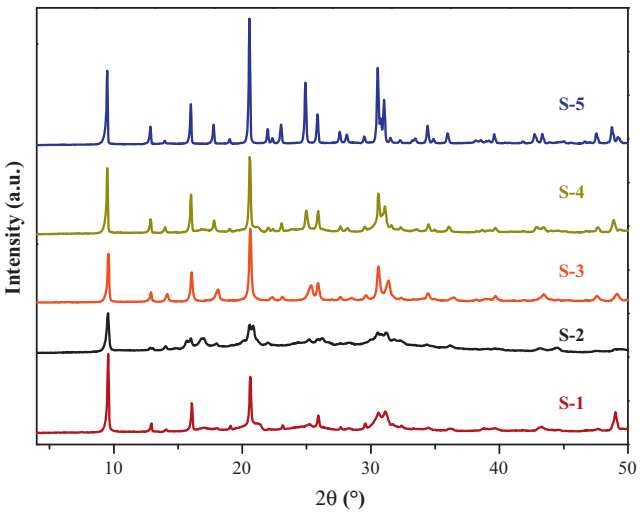

Fig. 1. XRD patterns of as-synthesized samples.

Comparison of XRD patterns of different samples evidences that there are some differences in peak width. In particular, sample S-2 (synthesized with TEAOH) exhibits the least intense reflections and a relatively ill-defined pattern. This fact suggests that sample

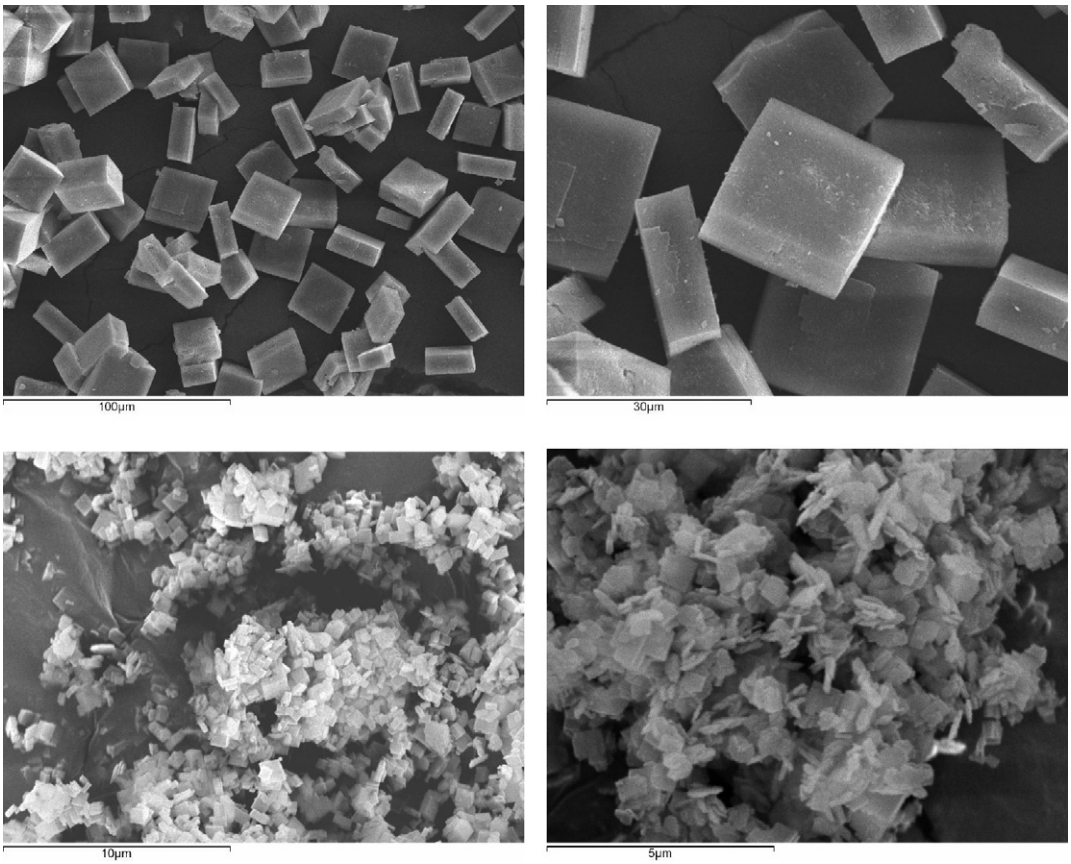

Fig. 2. SEM images of calcined samples, S-4 (top) and S-2 (bottom).

Table 2
Textural properties of calcined materials.

Sample	Surface area (m^2/g)			Pore volume (cm^3/g)		
	S_{micro}	S_{ext}	S_{total}	V_{micro}	V_{ext}	V_{total}
S-1	611	0	609	0.26	0.09	0.35
S-2	608	44	652	0.26	0.29	0.55
S-3	571	12	583	0.24	0.10	0.34
S-4	657	0	649	0.27	0.06	0.33
S-5	543	12	555	0.23	0.08	0.31

prepared with tetraethylammonium hydroxide could present crystal size significantly smaller than the rest of samples.

Some selected scanning electron microscopy (SEM) photographs of SAPO-34 materials synthesized with two different templates are presented in Fig. 2. In the case of sample S-4, synthesized with DPR, the typical cubic-like rhombohedra morphology can be clearly observed, which is quite similar to natural chabacite. The average crystal size of prisms is approximately 20 μm × 20 μm × 5 μm. Similar morphology is observed for samples S-1, S-3 and S-5 (Supplementary information, Fig. II). However, sample S-2, synthesized with TEAOH presents a quite different crystal shape and size. As it can be observed in the micrograph (Fig. 2), sample S-2 presents small plate-like crystals with smaller size, around 0.5 μm × 0.3 μm. These observations are in good agreement with XRD data previously presented, confirming the smaller crystal size of sample S-2.

3.2. Textural properties

Calcined materials were analysed by nitrogen adsorption–desorption at 77 K in order to determine their textural properties. All the samples present type I isotherms (according to the IUPAC classification [22]), corresponding to microporous materials (Fig. III in Supplementary information). Data of pore volume and surface area calculated from the isotherms are collected in Table 2. It can be observed that all the samples have surface area in the range 550–650 m^2/g. The sample with larger crystal sizes possess similar pore volume, around 0.35 cm^3/g, negligible values of external surface area and very low non-microporous pore volume. Only sample S-2, synthesized with TEAOH and having small crystal size, presents higher value of pore volume (0.55 cm^3/g), non-microporous pore volume (0.29 cm^3/g) and external surface (44 m^2/g). These differences can be explained in base to the smaller crystal size and the higher intercrystalline porosity.

3.3. Thermogravimetric and elemental analysis

Thermogravimetric analyses (TGA) were performed aiming to verify the incorporation of the SDA molecules in the structure of the as-made samples and their subsequent complete elimination after calcination prior to the use of SAPO-34 materials in the catalytic reactions. The TGA profiles of the samples studied are plotted in Fig. 3. These results show three different weight loss steps. The first weight loss (I), at temperatures below 473 K, can be attributed to adsorbed water desorption. The second weight loss (II), between 473 and 823 K, is due to the decomposition of the template. Finally, the third weight loss (III), at temperatures higher than 823 K, is associated with the further removal of organic residues occluded in the channels and cages of the SAPO-34 caused by oxygen combustion. Data of the different weight losses are presented in Table 3.

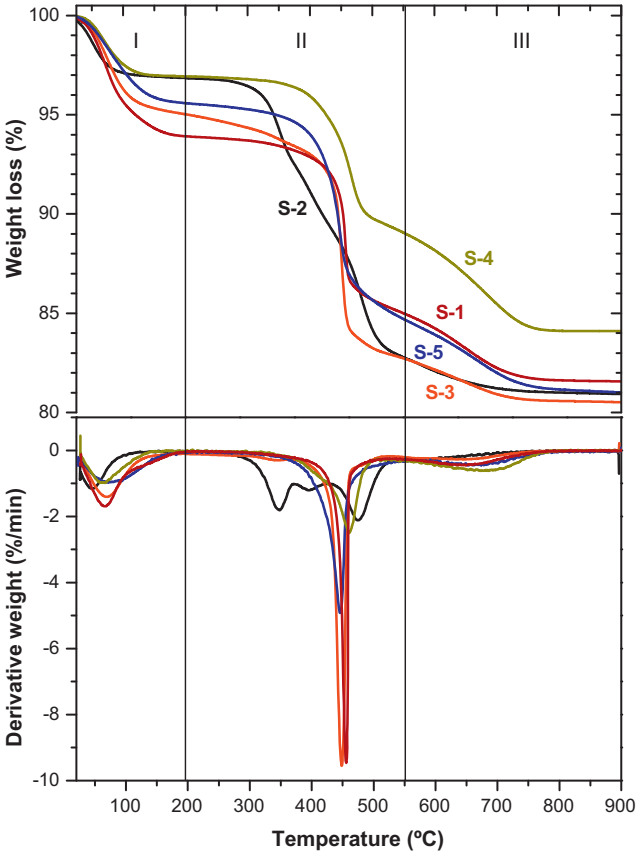

Fig. 3. Thermo gravimetric analyses (up) and derivative thermal analyses (down) of the different as-synthesized samples.

From the derivative plot presented in Fig. 3, it can be observed that the decomposition of the template occurs in a different way for sample S-2. While for the rest of the samples the decomposition process is associated to a single peak centred at 723 K, for S-2 the decomposition occurs in, at least, three different steps, beginning at ca. 623 K and finishing at ca. 773 K. The fact that the template decomposition began at lower temperature in this sample could be

Table 3
Elemental (CNH) and thermogravimetric analyses of the as-synthesized samples.

Sample	Weight loss (%)[a]			Organic content[b]			
	I	II	III	wt%	C/N		Moles of template per cage
	<473 K	473 K–823 K	>823 K		Exper.	Theor.	
S-1	6.2	8.7	3.6	11.3	5.1	6	1.0
S-2	3.1	14.2	1.8	13.9	7.3	8	1.0
S-3	5.0	12.1	2.4	13.0	5.6	8 (TEAOH) 1 (MA)	1.2 (0.76 TEAOH; 0.39 MA)
S-4	3.1	7.6	5.2	11.7	5.3	6	1.0
S-5	4.7	11.0	3.5	13.1	3.7	4	1.6

[a] From TGA analyses.
[b] From chemical analyses.

Table 4
Elemental composition.

Sample	Molar composition	$Si/(Al+P)_{gel}$	$Si/(Al+P)_{solid}$	Si incorporation[a]
S-1	$Si_{0.14}Al_{0.48}P_{0.38}O_2$	0.17	0.16	0.98
S-2	$Si_{0.17}Al_{0.43}P_{0.40}O_2$	0.15	0.21	1.31
S-3	$Si_{0.13}Al_{0.45}P_{0.41}O_2$	0.15	0.15	0.85
S-4	$Si_{0.13}Al_{0.47}P_{0.40}O_2$	0.15	0.15	1.00
S-5	$Si_{0.16}Al_{0.56}P_{0.24}O_2$	0.17	0.20	1.21

[a] The level of silicon incorporation is defined as the molar ratio of: $[Si/(Si+Al+P)_{solid}]/[Si/(Si+Al+P)_{gel}]$.

possibly attributed to its smaller crystal size and the lesser diffusional problems derived from it. However, it cannot be excluded that this effect be also due to a different mechanism of decomposition of the quaternary ammonium template respect to amines.

When the weight losses determined by TGA associated to the template elimination (steps II and III) are compared with the results of the organic content obtained from CHN elemental analyses (Table 3), a nice correlation is observed, confirming the previous weight losses assignment. The results obtained with both techniques were in good agreement. Moreover, the experimental C/N ratios determined for the different samples were very similar to the calculated theoretical values. This represents an additional evidence of the incorporation of the SDA to the zeolitic structure. Sample S-3, synthesized with two templates, presents a C/N ratio intermediate between the ratios which correspond to the two structure directing agents used. From this ratio it is possible to estimate the relative proportion of each SDA which is incorporated to the structure of the SAPO-34, being close to two TEAOH molecules per one MA molecule (Table 3).

Based on the topological structure of SAPO-34 molecular sieve, the average number of template molecules per cage in the different samples was calculated (Table 3). For samples synthesized with the bulkier templates (TEAOH, DPR and TEA), one molecule of SDA per unit cell is incorporated to the solid. Sample S-5, synthesized with the smaller template, is able to incorporate more than 1.5 molecules of DEA per unit cell.

The chemical composition of samples obtained by ICP-OES is presented in Table 4. In all the cases, the Si/Al + P ratio of the samples is close to that of the synthesis gels, although this value is slightly higher for samples synthesized with tetraethyl ammonium hydroxide (S-2) and diethyl amine (S-5).

3.4. ^{29}Si MAS NMR

The incorporation of Si to the SAPO-34 framework has been studied by ^{29}Si MAS NMR (Fig. 4). It has been described that when the amount of silicon incorporated to the SAPO framework is low, Si atoms are located in a unique Si(4Al) environment resulting from the substitution of phosphorous by silicon in the aluminophosphate framework [23]. However, if the silicon content is higher, multiple silicon environments can occur. This can be observed in Fig. 4, where various distinct positions can be distinguished in the range −89 to −110 ppm, attributed to Si(nAl) environments ($n = 0$–4), as shown in the figure. It is important to notice that sample S-2 presents a clearly different spectrum than the other four samples. Samples S-1, S-3, S-4 and S-5 present only a broad band centred at −89 ppm attributed to Si(4Al) environments, indicating that the Si atoms are in phosphorous positions, and therefore the silicon substitution is occurring solely via mechanism 2 (SM2: a phosphorous atom substituted by a silicon atom). This mechanism leads to Si surrounded by 4 Al atoms in the second coordination shell, and creates a negative charge per every Si atom in the framework, which is usually balanced by the positive charge of the organic molecules occluded within the microporous structure. However, in the case of sample S-2, in addition to this band, centred at −89 ppm,

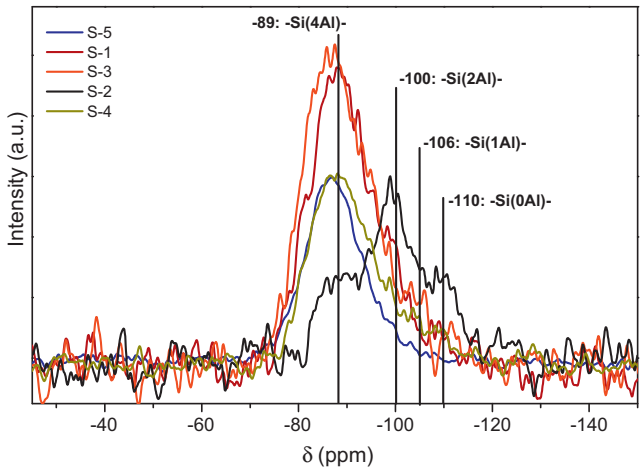

Fig. 4. ^{29}Si CP/MAS NMR spectra of the calcined samples.

at least three new bands can be clearly observed at −100, −106 and −110 ppm, which have been previously attributed to Si(2Al), Si(1Al) and Si(0Al), respectively. The presence of these bands can be explained if the silicon is incorporated into the framework via substitution mechanism 3 (SM3), in which the incorporation of Si occurs via a simultaneous substitution of a pair of adjacent Al and P atoms by two Si atoms. Due to the instability of Si–O–P bonds, this mechanism is always accompanied by a certain extent of SM2 substitution, thus giving rise to aluminosilicate domains (commonly referred to as Si islands) in the SAPO network. The simultaneous occurrence of both mechanisms results in the presence of different Si environments Si(nAl), where n varies between 1 and 3 at the border of the Si island. Depending on the ratio of SM3 to SM2 substitutions, the size and concentration of the Si islands will be different [24–26]. Some authors have proposed that the strength of the acid sites generated at the border of the Si islands is higher than that of the acid sites created by the isolated Si atoms, and that the strength increases as the value of n in the $Si(OAl)_n(OSi)_{4-n}$ environments decreases [24]. Thus, a higher number of acid sites are generated through the SM2 mechanism, while substitution via SM2 + SM3 yields less but stronger acid sites. The control of Si incorporation through the different mechanisms would therefore enable to modulate the acidity of these materials, which would affect catalytic behaviour. The different Si distribution that we have observed for sample S-2 could be attributed to its higher Si content, as it would favour the formation of silicon islands. Nonetheless, it has been shown that template properties such as size and morphology strongly affect the Si distribution in SAPO-34 [13]. Therefore, it can be speculated that TEAOH is the template that tend to promote most the substitution mechanism SM3.

3.5. Acidity

The FTIR spectrum in the OH stretching region (ν_{OH}) of the samples outgassed at 823 K is shown in Fig. 5. At 3747 and 3677 cm^{-1} two very week bands can be observed which are attributed to Si–OH and P–OH species located on the external surface of the sample particles, respectively. Sample S-2 presents a more intense peak at 3747 cm^{-1}, indicating the presence of an important amount of terminal silanols in this sample, which could be explained in base to its higher external surface. Two additional peaks with intense adsorption and maxima at 3630 and 3600 cm^{-1} can also be observed for all the samples. These bands correspond to bridging hydroxyl groups (Si–OH–Al) associated to the Brönsted acid centres of these materials [27–32]. These hydroxyls have been also named respectively species A and C (OH_A, OH_C) in the literature and they

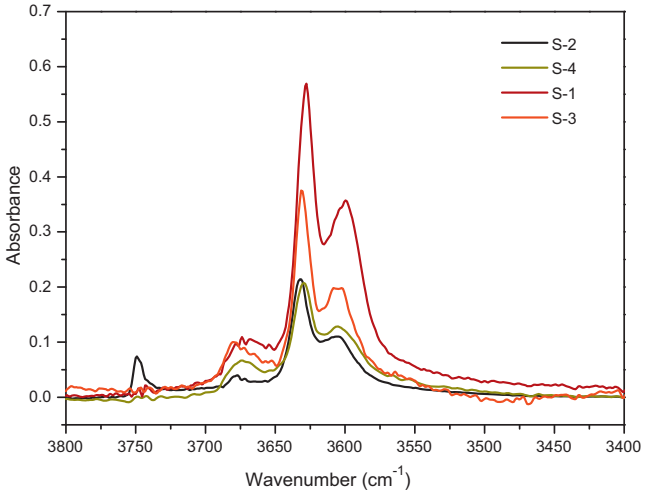

Fig. 5. Normalized FTIR spectra of calcined samples outgassed at 823 K.

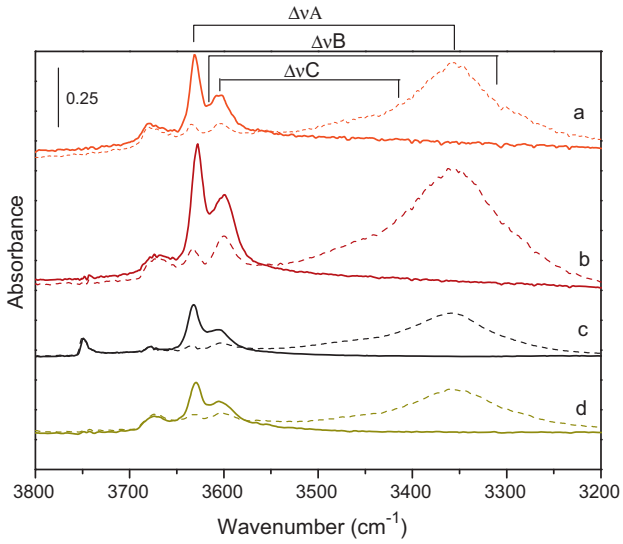

Fig. 6. Normalized FTIR spectra of calcined samples (a) S-3 (TEAOH and MA), (b) S-1 (TEA), (c) S-2 (TEAOH) and (d) S-4 (DPR) outgassed at 823 K (solid lines) and in contact with 0.25 mbar CO (dotted lines). Spectra were recorded at 77 K.

were explained in terms of different crystallographic positions [32,33].

The type of template used in the synthesis was shown to affect the population of acid sites. Sample obtained with triethyl amine (S-1) exhibited the highest content of hydroxyl groups, while sample synthesized with tetraethyl ammonium hydroxide (S-2) displayed the lowest content of them.

A higher number of acid sites are generated in samples S-1 and S-3, through silicon substitution mechanism SM2, as compared to sample S-2 for which both mechanisms, SM2 and SM3, take place. The simultaneous occurrence of both mechanism results in the presence of silicon islands that give rise to stronger acid sites than those associated to the isolated Si species created via mechanism SM2. Therefore the sample prepared with tetraethyl ammonium hydroxide (S-2) possessed the lowest content of acid sites but with an expected higher average strength.

In order to characterize the strength of the acid centres, experiments of adsorption of a weak base (CO) have been carried out. CO can react with acidic OH species forming an OH···CO adduct. This H-bonding interaction produces a frequency shift, large broadening and increase of intensity of bands corresponding to acidic OH species [34–36]. Therefore, the adsorption of increasing amounts of CO progressively erodes the infrared bands in the region 3630–3600 cm^{-1} and gives rise to the development of new bands at approximately 3300–3400 cm^{-1}. Fig. 6 presents the FTIR spectra of the different samples before and after CO adsorption (0.25 mbar) at 77 K. The shift of bands revealed a third component (OH_B) at ca. 3610 cm^{-1} (Fig. 6), which exhibited the strongest acidity (largest band shift), assigned to OH groups in the border of silicon islands. The magnitude of the batochromic shift produced for component B upon CO adsorption (around 320 cm^{-1}) is similar to that observed for Brönsted sites in H-ZSM-5 (335 cm^{-1}). This is an indication of the strong acid character of OH_B sites compared to components A and C, which presented a milder acidity [30]. Although the large band width of these bands makes band deconvolution results rather unreliable, a tentative deconvolution of these bands suggests that the percentage of the B type acid centres is higher for sample S-2, synthesized with TEAOH.

3.6. Catalytic activity

The catalytic activity of these materials in the MTO reaction was studied at 673–723 K and different WHSV, as it has been described previously in Section 2.

When high temperature and high WHSV conditions (723 K and 14.2 h^{-1}, respectively) are used, the catalysts deactivate very rapidly (Table 5). Although at the initial stage of the reaction (5 min of time-on-stream) all the catalysts present a complete conversion of methanol and high selectivity towards short chain

Table 5
Results of the MTO reaction carried out with the different samples. Selectivity and methanol conversion (%) vs. time-on-stream (TOS).

Sample	S-1		S-2		S-3		S-4		S-5	
TOS (min)	5 min	60 min	5 min	60 min	5 min	60 min	5 min	60 min	5 min	60 min
Methane	1.5	0.2	2.6	1.7	1.2	0.1	2.7	0.3	2.3	0.2
Ethylene	37.2	0.2	42.6	20.8	39.8	0.8	47.0	0.2	28.6	0.1
Ethane	1.2	0	0.4	0.1	0.8	0	2.2	0	2.7	0
Propylene	32.6	0.2	32.6	20.2	37.7	0.9	34.7	0.1	21.8	0.1
Propane	0	0	2.1	0	0.4	0	2.5	0	0.2	0
Dimethyl ether	18.4	98.6	0.1	49.6	8.1	97.5	1.4	98.0	39.8	99.0
1-Butene + iso-butene	2.4	0	3.0	1.8	2.3	0.2	2.3	0.5	1.0	0
n-Butane	0	0	0.2	0	0.7	0	0.4	0	0.2	0
Trans-2-butene	3.4	0	3.8	2.8	4.5	0.1	3.7	0	1.8	0.2
Cis-2-butene	1.7	0	2.8	1.4	2.2	0.1	1.9	0	0.8	0
C_5–C_7	1.5	0.2	3.7	1.0	2.1	0.1	1.2	0.3	0.5	0
C_8+	0.1	0.6	6.2	0.6	0.4	0.3	0.1	0.5	0.3	0.5
Methanol conversion	89.9	45.0	99.2	80.8	95.2	68.1	98.5	28.0	78.5	64.7

Test conditions: WHSV = 14.22 h^{-1}, T = 723 K, catalyst weight = 0.5 g.

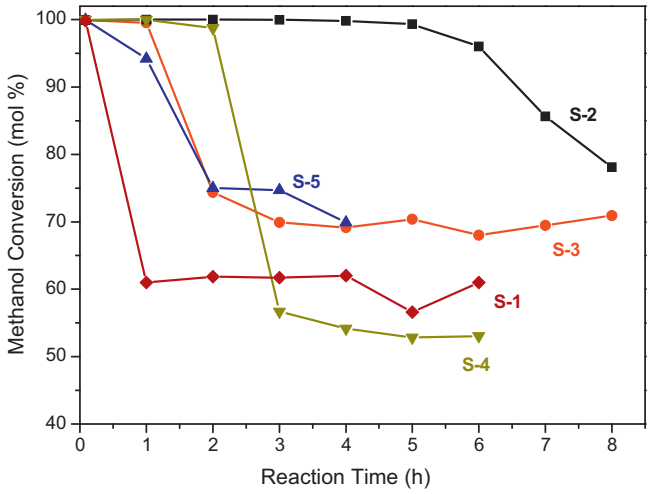

Fig. 7. Methanol conversion vs. time-on-stream for the different samples. Experimental conditions: WHSV = 1.2 h^{-1}, T = 673 K, catalyst weight = 1.0 g.

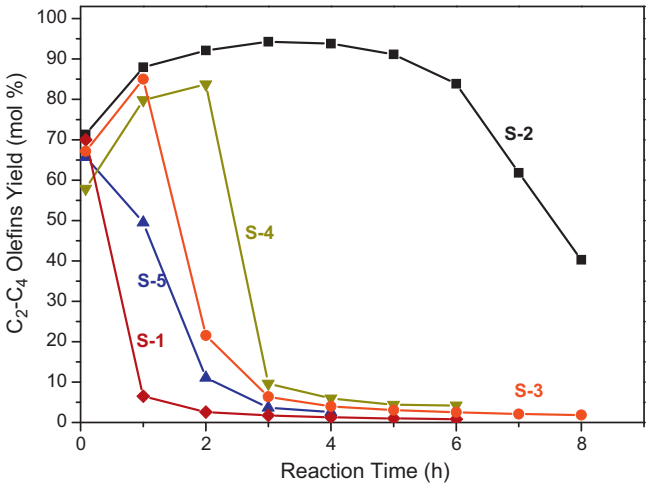

Fig. 8. Selectivity to short chain olefins (C_2–C_4) in function of the time on stream for the different samples in the MTO reaction. Experimental conditions: WHSV = 1.2 h^{-1}, T = 673 K, catalyst weight = 1.0 g.

olefins (C_2–C_4), after 1 h of TOS, the catalysts deactivate and the conversion decreases appreciably. In the case of samples S-1 and S-4 methanol conversion goes down to less than 50%, samples S-3 and S-5 to ca. 65% and only sample S-2, synthesized with TEAOH, maintains the conversion above 80%, although the selectivity to C_2–C_4 olefins decreases from 85% to 47%. All the catalysts, after 1 h of TOS present a high selectivity to dimethyl ether (DME), primary product of the reaction which can be easily obtained from methanol dehydration by using catalysts with lower acidity, such as γ-Al_2O_3 [37]. This high proportion of DME after a short reaction time, can be attributed to the selective deactivation of the stronger acid centres of the catalysts, which are able to produce the dehydration of DME to render the short chain olefins.

As it was mentioned previously, the main problem of this kind of catalyst in the MTO process is the rapid deactivation attributed to the deposition of high molecular weight hydrocarbons on the pore entrances. In this study, sample S-2 synthesized with tetraethyl ammonium hydroxide, under the experimental conditions explored, presents an improved stability in this reaction. This can be attributed to two different factors: first, the smaller crystal size and high external surface which allows the rapid diffusion of the products to the reaction media, avoiding subsequent transformations of the olefins to heavier products which deactivate the catalyst; second, the presence of stronger acid centres in this sample as suggested by ^{29}Si MAS NMR and FTIR characterization. Both parameters can justify the higher stability of this sample.

In order to compare all the catalysts under more favourable conditions, experiments with a lower WHSV have been carried out. Results of conversion and selectivity to C_2–C_4 olefins are presented in Figs. 7 and 8. Again, sample S-2 presents the best results in terms of stability and selectivity. While samples S-1, S-3, S-4 and S-5 render methanol conversions below 70% after not more than 2 h of TOS, sample S-2 is able to maintain the total conversion of methanol for more than 5 h (Fig. 7). In addition, sample S-2 presents a much higher selectivity to short chain olefins during the overall reaction test, obtaining values above 90% for up to 6 h of TOS (Fig. 8). The rest of catalysts only produce DME after 3 h of TOS, due to the complete deactivation of the strongest acid centres. The combination of high external surface and small crystal size, facilitating the accessibility of the reactant molecules to the acid sites, together with the stronger acidity of sample S-2 could be the reasons to explain the better catalytic performance of this catalyst prepared with tetraethylammonium hydroxide.

4. Conclusions

SAPO-34 molecular sieves synthesized with different structure directing agents are shown to exhibit different physicochemical properties, especially textural parameters and particle size. These catalysts exhibited a high activity in the MTO process, with high selectivity to short chain olefins, at the initial stages of the reaction, but they deactivated rapidly with time-on-stream, especially when the reaction was carried out at high space velocity. The external surface, crystal size and acidity strongly influenced the activity, selectivity and lifetime of the different catalysts. The sample synthesized with tetraethylammonium hydroxide as structure directing agent has rendered the best catalytic performance based on its higher external surface, smaller crystal size and higher acidity.

Acknowledgements

This work has been supported by the Spanish Ministry of Science and Innovation, project MAT2009-13569. TA acknowledges CSIC for a JAE PhD grant. Authors acknowledge Prof. Barbara Onida and Dr. Manuel Sánchez-Sánchez for the helpful discussions on the FTIR and NMR data, and the Analytical Support Unit of the ICP for collecting the characterization data.

Appendix A. Supplementary data

Supplementary data associated with this article can be found, in the online version, at doi:10.1016/j.cattod.2011.07.038.

References

[1] G.A. Olah, A. Goeppert, G.K.S. Prakash, J. Org. Chem. 74 (2) (2009) 487–498.
[2] C. Song, Catal. Today 115 (2006) 2–32.
[3] C.N. Hamelinck, A.P.C. Faaij, J. Power Sources 111 (1) (2002) 1–22.
[4] S.L. Meisel, J.P. McCullough, C.H. Lechthaler, P.B. Weisz, Chemtech 6 (1976) 86–89.
[5] M. Bjorgen, S. Svelle, F. Joensen, J. Nerlov, S. Kolboe, F. Bonino, L. Palumbo, S. Bordiga, U. Olsbye, J Catal. 249 (2) (2007) 195–207.
[6] A.G. Gayubo, A.T. Aguayo, M. Olazar, R. Vivanco, J. Bilbao, Chem. Eng. Sci. 58 (23–24) (2003) 5239–5249.
[7] D. Chen, K. Moljord, T. Fuglerud, A. Holmen, Micropor. Mesopor. Mater. 29 (1999) 191–203.
[8] S. Wilson, P. Barger, Micropor. Mesopor. Mater. 29 (1999) 117–126.
[9] M. Popova, C. Minchev, V. Kanazirev, Appl. Catal. A: Gen. 169 (1998) 227–235.
[10] J. Liang, H.-Y. Li, S-Q. Zhao, W.-G. Guo, R.-H. Wang, M.-L. Uing, Appl. Catal. 64 (1990) 31–40.

[11] H.O. Pastore, S. Coluccia, L. Marchese, Annu. Rev. Mater. Res. 35 (2005) 351–395.
[12] B.M. Lok, T.R. Cannan, C.A. Messina, Zeolites 3 (1983) 282–291.
[13] R. Vomscheid, M. Briend, M.J. Peltre, P.P. Man, D. Barthomeuf, J. Phys. Chem. 98 (1994) 9614–9618.
[14] Y.-J. Lee, S.-C. Baek, K.-W. Jun, Appl. Catal. A: Gen. 329 (2007) 130–136.
[15] L. Ye, F. Cao, W. Ying, D. Fang, Q. Sun, J. Porous Mater. 18 (2011) 225–232.
[16] G. Liu, P. Tian, J. Li, D. Zhang, F. Zhou, Z. Liu, Micropor. Mesopor. Mater. 111 (2008) 143–149.
[17] B.M. Lok, C.A. Messina, R.L. Patton, R.T. Gajek, T.R. Cannan, E.M. Flanigen, US Patent 4,440,871 (1984).
[18] E. Dumitriu, A. Azzouz, V. Hulea, D. Lutic, H. Kessler, Micropor. Mater. 10 (1997) 1–12.
[19] Y.Y. Zheng, T.L. Yang, X.H. Zhou, S.K. Shen, J. Fuel Chem. Technol. 27 (1999) 139.
[20] J. Tan, Z.M. Liu, X.H. Bao, X.C. Liu, X.W. Han, C.Q. He, R.S. Zhai, Micropor. Mesopor. Mater. 53 (2002) 97–108.
[21] Ø.B. Vistad, D.E. Akporiaye, F. Taulelle, K.P. Lillerud, Chem. Mater. 15 (2003) 1639–1649.
[22] K.S.W. Sing, D.H. Everett, R.A.W. Haul, L. Moscou, R.A. Pierotti, J. Rouquerol, T. Siemieniewska, Pure Appl. Chem. 57 (1985) 603–619.
[23] C.S. Blackwell, R.L. Patton, J. Phys. Chem. 88 (1984) 6135–6139.
[24] S. del Val, T. Blasco, E. Sastre, J. Pérez-Pariente, J. Chem. Soc., Chem. Commun. (1995) 731–732.
[25] J.A. Martens, C. Janssens, P.J. Grobet, H.K. Beyer, P.A. Jacobs, Stud. Surf. Sci. Catal. 49 (1989) 215–225.
[26] A.M. Prakash, S. Unnikrishnan, K.V. Rao, Appl. Catal. A: Gen. 110 (1994) 1–10.
[27] L. Marchese, J. Chen, P.A. Wright, J.M. Thomas, J. Phys. Chem. 97 (1993) 8109.
[28] L. Smith, A.K. Cheetham, L. Marchese, J.M. Thomas, P.A. Wright, J. Chen, E. Gianotti, Catal. Lett. 41 (1996) 13–16.
[29] K. Góra-Marek, M. Dereinski, P. Sarv, J. Datka, Catal. Today 101 (2005) 131–138.
[30] G.A.V. Martins, G. Berlier, S. Coluccia, H.O. Pastore, G.B. Superti, G. Gatti, L. Marchese, J. Phys. Chem. C 111 (2007) 330–339.
[31] S. Coluccia, L. Marchese, G. Martra, Micropor. Mesopor. Mater. 30 (1999) 43–56.
[32] L. Smith, L. Cheetham, L. Marchese, E. Gianotti, J.M. Thomas, P.A. Wright, J. Chen, Catal. Lett. 41 (1996) 13–16.
[33] A. Albuquerque, S. Coluccia, L. Marchese, H.O. Pastore, Stud. Surf. Sci. Catal. 154 (2004) 966–970.
[34] A. Zecchina, S. Bordiga, G. Spoto, D. Scarano, G. Petrini, G. Leofanti, M. Padovan, J. Chem. Soc., Faraday Trans. 88 (1992) 2959–2969.
[35] L. Kustov, V. Kazansky, S. Beran, L. Kubelková, P. Jiru, J. Phys. Chem. 91 (1987) 5247–5251.
[36] L. Kubelková, S. Beran, J.A. Lecher, Zeolites 9 (1989) 539–543.
[37] S.-M. Kim, Y.-J. Lee, J.W. Bae, H.S. Potdar, K.-W. Jun, Appl. Catal. A: Gen. 348 (2008) 113–120.